approximation agree well with experiment. It appears the correlation and relativistic effects can be ignored. They are either small or somehow the Slater exchange approximation accounts for them. This compensation is not as strange as it may at first appear. For example the use of free atomic potentials with Kohn-Sham exchange produces Γ-point eigenvalues very near the SCOPW values using Slater's exchange term.

The agreement with experiment would be outstanding if one reinterpreted the photoemission results as was discussed in Sec. III. That is one has three conduction-band minima; the lowest minimum occurs at the Γ point; the next higher minimum is located at L, 0.38 eV above the Γ-point minimum; and the third minimum is located on the symmetry line Δ, occurring 0.82 of the way from Γ to X at an energy value of 0.82 eV above the Γ-point minimum. However, the SCOPW model does not give any identification to the structure observed by James *et al.*[22] Aside from this everything else fits, even the ratio of the effective masses of the Γ and L minima calculated along Λ agree well with estimates used in transport calculations.

If one assumes that the location of the X_{1c} and L_{1c} are correctly given by Ref. 5, one finds that the direct energy differences (values located at the same k value in the Brillouin zone) are very close to experiment, while the indirect energies are correct only to about 0.5 eV. If this is true this discrepancy is thought to be related to the fact that the model uses a local exchange approximation.

Note added in proof. The many-body work of L. Hedin, S. Lundquist, and B. Lindquist support the use of Slater's exchange in deriving excitation energies.[32]

[32] See review article by L. Hedin and S. Lindquist, in *Solid State Physics*, edited by F. Seitz and D. Turnbull (Academic Press Inc., New York, to be published).

PHYSICAL REVIEW B VOLUME 1, NUMBER 2 15 JANUARY 1970

Low-Temperature Non-Ohmic Electron Transport in GaAs

RICHARD S. CRANDALL
RCA Laboratories, Princeton, New Jersey 08540
(Received 17 January 1969; revised manuscript received 18 July 1969)

The electric field dependence of the electrical conductivity and Hall effect in n-type epitaxial GaAs crystals was measured between 1.2 and 300°K. Some of the samples showed donor freeze-out, while others showed none down to the lowest temperatures. The non-Ohmic transport below 77°K was explained by a theory that included ionized-impurity and acoustic-phonon scattering, where the electron-phonon interaction was assumed to involve screened piezoelectric and deformation potentials. A treatment assuming an electron temperature and a second theory involving a direct calculation of the electron distribution function were compared with experiment. Only the theory involving a direct distribution-function calculation appears to explain the observations. A new model was proposed for the current-controlled negative resistance observed at low temperatures. This model depends upon the screening of impurity scattering and the electron-phonon interaction.

I. INTRODUCTION

A SUBJECT which has been studied in detail is non-Ohmic transport and the behavior in Ge at high electric fields, for example, is well understood.[1,2] The interaction of the electrons with phonons plays an important role in such studies. In GaAs, however, there are electron-phonon interactions not found in Ge. There is a strong polar interaction with the optical phonon. Furthermore, the absence of a center of inversion symmetry permits a strong interaction with acoustic phonons via the piezoelectric coupling.

Considerable effort has been devoted to the study, in the vicinity of room temperature, of non-Ohmic transport in the region near and above the Gunn effect field.[3,4] However, because of the strong interaction between electrons and optical phonons, other interactions may be neglected in explaining the observed behavior. There has been less investigation at low temperatures,[5–8] where other interactions are important. Oliver[6,7] analyzed his low-temperature non-Ohmic transport measurements by assuming the electron energy distribution was Maxwellian with an electron temperature different from the lattice temperature. This model is the electron-temperature model (ETM).[9] He assumed that acoustic- and optical-phonon

[1] E. G. S. Paige, in *Progress in Semiconductors*, edited by A. F. Gibson and R. E. Burgess (John Wiley & Sons, Inc., New York, 1964), Vol. 8, Chap. 6.
[2] E. M. Conwell, in *Solid State Physics*, edited by F. Seitz, D. Turnbull, and H. Ehrenreich (Academic Press Inc., New York, 1967), Suppl. 9, Chap. 2.
[3] J. B. Gunn, Solid State Commun. **1**, 88 (1963).
[4] Reference 2, pp. 80–99.
[5] R. A. Reynolds, Solid State Electron. **11**, 385 (1968).
[6] D. J. Oliver, Phys. Rev. **127**, 1045 (1962).
[7] D. J. Oliver, in *Proceedings of the International Conference on the Physics of Semiconductors. Exeter, July, 1962*, edited by A. C. Strickland (The Institute of Physics and The Physical Society, London, 1962), p. 133.
[8] R. S. Crandall and P. Gwozdz, Bull. Am. Phys. Soc. **13**, 406 (1968).
[9] R. Stratton, Proc. Roy. Soc. (London) **A242**, 355 (1957).

scattering were the principle energy loss mechanisms and that ionized-impurity scattering was responsible for the momentum relaxation. In the high-field region, where optical phonon dominates acoustic-phonon scattering, he found quantitative agreement with experiment. At low fields, where acoustic-phonon scattering is the most important energy loss, he obtained only qualitative agreement with experiment. He also showed theoretically that piezoelectric scattering was the most important energy loss process below 30°K. At low temperatures, a current-controlled negative resistance has been observed by Oliver,[6] Reynolds,[5] and Stillman *et al.*[10]

In this paper we shall give a quantitative analysis of the Ohmic and non-Ohmic transport in the low-field region. This electron transport will be shown to be determined by ionized-impurity and acoustic-phonon scattering, where the acoustic phonons interact with the electrons via both the piezoelectric and deformation potentials. A direct solution of the Boltzmann equation (BES),[11] involving the above scattering mechanisms, is used to analyze the non-Ohmic transport. The observed current-controlled negative resistance will be analyzed by a new model involving screening of impurity scattering and the electron-phonon interaction.

II. APPARATUS

All samples were epitaxially grown,[12] undoped, n-type single-crystal GaAs. Hall samples were $10\times5\times0.1$ mm, with indium contacts alloyed in 0.3-mm-diam holes that were sandblasted in the crystal. The current contacts were 8 mm apart on a line through the center of the crystal. The voltage contacts were at the corners of a square, which was 2.5 mm on an edge and centered in the middle of the crystal. The electric field was applied in the ⟨100⟩ direction to minimize the acoustoelectric interaction. The sample and a Ge thermometer were mounted in a copper can containing helium exchange gas which provided a nearly isothermal environment. This can, wound with a heater, was placed in a second exchange gas can immersed in liquid helium. The temperature could then be conveniently controlled between 1.2 and 40°K. Low-field Hall data were obtained by conventional dc methods using a high-impedance electrometer to measure Hall voltage, potential drop in the crystal, and current. Pulsed current techniques were used to avoid sample heating at high electric fields. The magnetic field was low enough to ensure that the Hall angle was less than 0.1 rad.

[10] G. E. Stillman, C. M. Wolfe, I. Melngailis, C. D. Parker, P. E. Tannenwald, and J. O. Dimmock, Appl. Phys. Letters **13**, 83 (1968).
[11] R. S. Crandall, Phys. Rev. **169**, 585 (1968).
[12] J. J. Tietjen and J. Amick, J. Electrochem. Soc. **113**, 724 (1966).

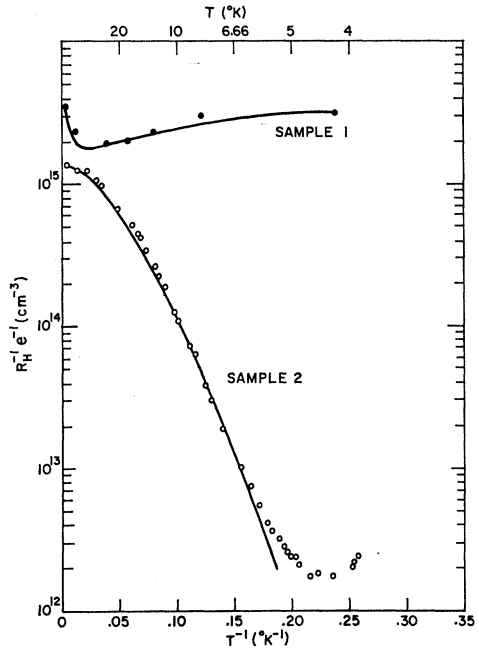

FIG. 1. Temperature dependence of $(eR_H)^{-1}$ which is proportional to the carrier density. The open circles are for the purest sample 2; the closed circles are for the impure sample 1. The solid curves are theory.

III. RESULTS

Hall-effect measurements were made on two groups of crystals: one that exhibited donor deionization and another that did not. In both classes of crystals, the donors are probably the same.

Figures 1–5 show the results of the Hall-effect measurements. The points are the experimental data; the curves are theoretical and will be discussed in Sec. IV.

Figure 1 shows the temperature dependence of the reciprocal of the product of the Hall constant R_H and the electronic charge e. Sample 1 is one of the

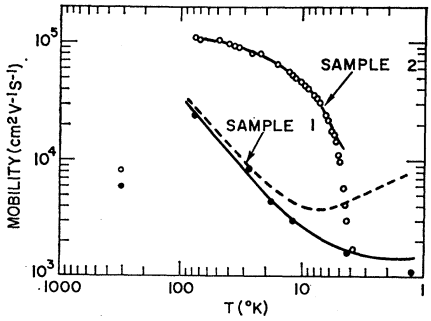

FIG. 2. Temperature dependence of the mobility for samples 1 and 2. The curves are theory and the points are data. The data and theory for sample 1 are the conductivity mobility. The data and theory for sample 2 are the Hall mobility. The solid and dashed curves for sample 1 represent two different choices for the screening density.

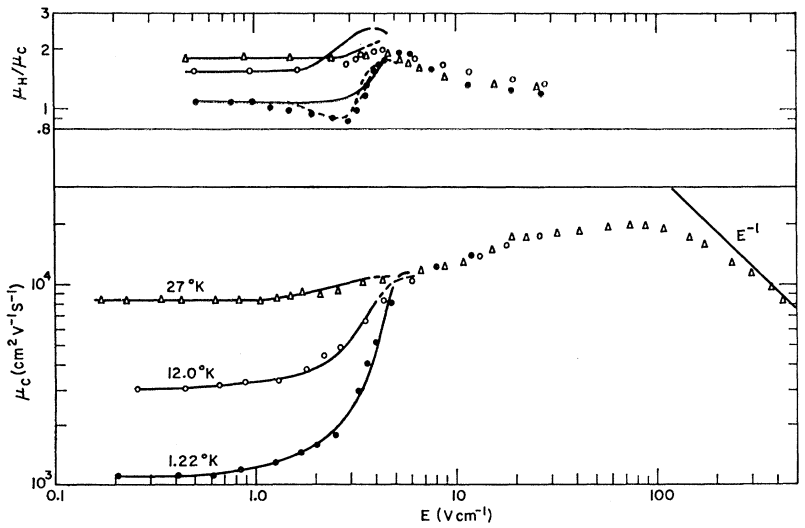

FIG. 3. The field dependence of the conductivity mobility and the ratio $\mu_H\mu_c^{-1}$ for the impure sample 1. The abscissas are the same for both plots. The top curves correspond to the temperatures shown on the μ_c plot. The lines are theory, with the broken portions at high field pertaining to the region where the effect of the optical phonon was approximated. The dashed and solid lines for the 1.22°K $\mu_H\mu_c^{-1}$ plot are for the two choices of screening length. The theoretical curve at 1.22°K is normalized to the Ohmic mobility data. The E^{-1} line is drawn for reference.

crystals which does not show donor deionization. Sample 2 clearly shows donor deionization.

In Fig. 2 the temperature dependence of the mobility is shown for the two samples. For sample 2 the Hall mobility μ_H is plotted, while for sample 1 it is the conductivity mobility μ_c which is plotted. The conductivity mobility was obtained by dividing the measured conductivity by the product of e and the carrier density n. The carrier density was determined on the assumption that $n=(R_He)^{-1}$ at room temperature, and that n was not a function of temperature for this sample class. This gives a carrier density of 3.5×10^{15} cm^{-3}. In Sec. IV we shall show that the assumption of a temperature-independent carrier density is consistent with the experimental results.

In Fig. 3 μ_c and the ratio $\mu_H\mu_c^{-1}$ for sample 1 are plotted versus electric field E at three sample temperatures. The values of the ratio $\mu_H\mu_c^{-1}$ were obtained from the measured values of R_H and the assumed carrier density of 3.5×10^{15} cm^{-3}, by using the relation

$$\mu_H/\mu_c\equiv R_Hne. \quad (1)$$

In Fig. 4 the field dependence of the Hall mobility is shown at different temperatures for the sample 2 that exhibits donor deionization. The qualitative behavior is similar to that shown for μ_c in Fig. 3. However, both the Ohmic and the maximum high-field mobilities are higher than for sample 1. The field dependence of μ_H near 1.8 V cm^{-1} at 5.12°K in sample 2 is characteristic of all our samples that show donor deionization. The mobility increases with *decreasing* electric field.

In Fig. 5 the electric field dependence of $(R_He)^{-1}$ is plotted for sample 2. These data are for the same temperatures as the Hall mobility curves in Fig. 4. The rapid increases in $(R_He)^{-1}$ and the Hall mobility take place in the same field region. The increase in $(R_He)^{-1}$ by an order of magnitude, shown by the dashed line, is accompanied by a 10% decrease in the field. This is the same region where the Hall mobility increases with decreasing field. The current density, which is $\mu_HE(R_H)^{-1}$, also increases with decreasing electric field in this field region. This behavior is typical of a current-controlled negative resistance.

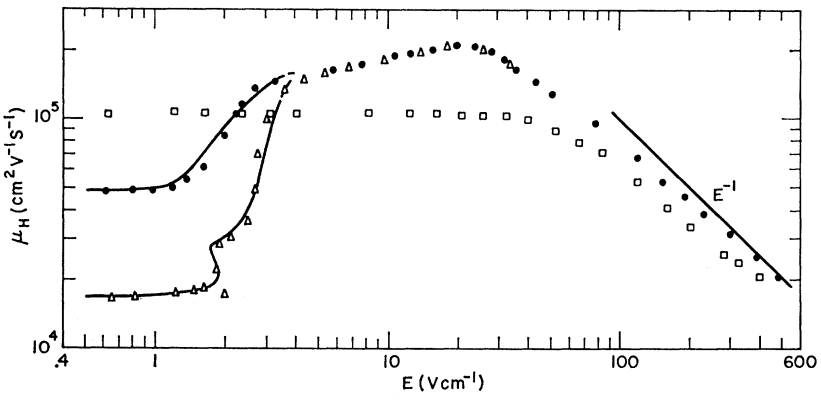

FIG. 4. Field dependence of the Hall mobility in sample 2 that shows donor deionization. The solid lines are theory. The E^{-1} line is for reference. Triangles: 5.12°K; closed circles: 11.8°K; open squares: 77°K.

IV. DISCUSSION

A. Ohmic Transport

1. Mobility

In pure GaAs we expect the mobility to be governed by optical- and acoustical-phonon scattering.[13] Since, in general, GaAs crystals contain appreciable impurity concentrations, ionized and neutral impurities contribute to the scattering. Ehrenreich[13] showed that above 77°K the mobility was dominated by optical-phonon and ionized-impurity scattering. Because the optical-phonon density decreases rapidly at low temperatures (the optical-phonon energy is about 420°K)[13] optical-phonon scattering is weak at low temperatures. Therefore, the low-temperature transport should be dominated by impurity and acoustic-phonon scattering. We shall compare our mobility data with a mobility calculation[11] which includes impurity and acoustic-phonon scattering. These calculated values are only reliable below 77°K, where optical-phonon scattering[13] contributes less than 10% to the measured mobility. Because of the high carrier density in sample 1, it is necessary to use Fermi statistics and include screening of the electron-phonon interaction. In the Appendix, we outline the modifications of the expressions in Ref. 11, hereafter referred to as I, made to include screening and Fermi statistics.

For ionized-impurity scattering, the momentum relaxation time as given by the Brooks-Herring expression[14] for a singly ionized impurity is

$$\frac{1}{\tau_i}=\frac{2\pi e^4 m^* N_I}{\kappa^2|\mathbf{K}|^3\hbar^3}\left[\ln\left(1+\frac{4|\mathbf{K}|^2}{K_s^2}\right)-\frac{1}{1+K_s^2/4|\mathbf{K}|^2}\right], \quad (2)$$

where N_I is the impurity density, κ is the dielectric constant, m^* is the band mass, $\mathbf{K}$ is the electron wave vector, and K_s is the screening wave vector which is given by the Thomas-Fermi expression[15]

$$K_s^2=[\pi ne^2/(2kkT)][F_{-1/2}(\eta)/F_{1/2}(\eta)], \quad (3)$$

where k is Boltzmann's constant, T is the electron temperature, and $F_{-1/2}(\eta)[F_{1/2}(\eta)]^{-1}$ is the ratio of the Fermi-Dirac integrals

$$F_\alpha(\eta)=\int_0^\infty x^\alpha dx/[\exp(x-\eta)+1], \quad (4)$$

where η is the Fermi energy divided by kT. The screening density is assumed to be the free carrier density. Admittedly, the Brooks-Herring expression, which uses the Born approximation to calculate the scattering cross section, is not an ideal treatment of the ionized-impurity scattering. Although there have been some improvements on the Born approximation,[16,17] the improvement does not appear to justify the mathematical complexity involved. Moore's[17] calculation is carried out only to the second Born approximation, and the partial-wave calculations[16] still use the Born approximation to treat the screening.[18] The inclusion of electron-electron (e-e) scattering is beyond the scope of this paper. Its inclusion would make the problem inordinately complex to solve.[19] In the worst case which has been treated,[19] e-e scattering reduces the mobility by at most 40%. In our crystals $n<N_I$ and for this condition, the effect of e-e scattering on the mobility is considerably reduced. With the above reservations, we can see how well the theory agrees with experiment.

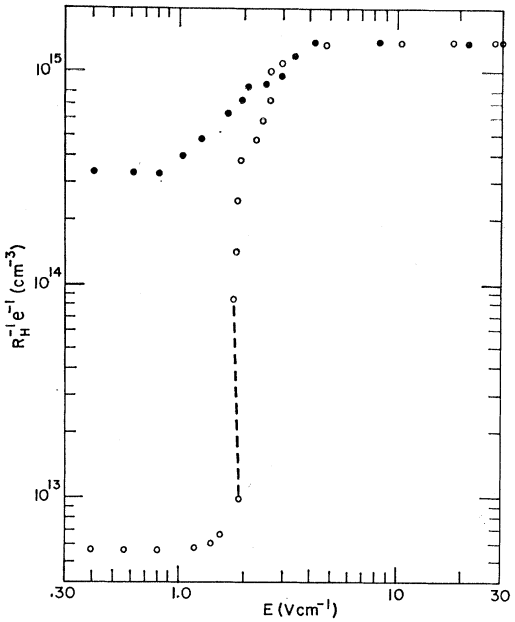

FIG. 5. Field dependence of $(R_He)^{-1}$ at 5.12°K (open circles) and 11.8°K (closed circles) for sample 2. The dashed line marks the negative resistance region.

To calculate μ_H and μ_c we use the expressions derived in I. In the low magnetic field limit, the parameter $\omega_0\tau_0$ can be set equal to zero in Eqs. (37)–(39) of I. The relaxation times for acoustic-phonon scattering via the deformation and piezoelectric potentials are given by Eqs. (26) and (27) of I, respectively. The total relaxation time that appears in Eqs. (37)–(39) of I is given in the usual manner by adding the reciprocals of the relaxation times for each scattering mechanism.

The mobility curves in Fig. 2 were calculated using the above procedure. The following parameters used

[13] H. Ehrenreich, Phys. Rev. **120**, 1951 (1960).
[14] H. Brooks, in *Advances in Electronics and Electron Physics*, edited by L. Marton (Academic Press Inc., New York, 1955) Vol. 7, pp. 156–160.
[15] A. C. Beer, in *Solid State Physics*, edited by F. Seitz and D. Turnbull (Academic Press Inc., New York, 1963), Suppl. 4, pp. 107–114.
[16] F. J. Blatt, J. Phys. Chem. Solids **1**, 262 (1957); J. B. Krieger and S. Strauss, Phys. Rev. **169**, 674 (1968).
[17] E. J. Moore, Phys. Rev. **160**, 618 (1967); **160**, 607 (1967).
[18] L. D. Landau and E. M. Lifshitz, *Statistical Physics* (Pergamon Press, Ltd., London, 1958), pp. 232–234.
[19] Reference 1, p. 84; J. Appel, Phys. Rev. **125**, 1815 (1962).

in this paper and I were chosen: $m^*=0.071m_e$[20]; $\kappa=12.5$[21]; the elastic moduli[22] $c_{11}=1.188$, $c_{12}=0.538$, and $c_{44}=0.594$ in units of 10^{12} dyn cm^2; the piezoelectric stress constant $h_{14}=1.57\times10^9$ V/m[23]; and the deformation potential $D=7$ eV.[13] The impurity density was taken equal to the density of acceptors N_A plus the density of ionized donors. Over most of the temperature range, ionized impurities dominate the scattering. Even though at 77°K in sample 2, where the mobility due to acoustic-phonon scattering is about ten times the mobility due to ionized-impurity scattering alone, the mobility calculated combining both scattering mechanisms is about 50% less than the mobility due only to ionized-impurity scattering. Acoustic-phonon scattering affects the mobility because in performing the average of the relaxation time the strong energy dependence of ionized-impurity scattering gives considerable weight to the phonon scattering. The measured mobility is less than the theoretical value below 5.5°K because of impurity conduction. In this region, the measured Hall mobility is always less than the conduction-band mobility.[24]

The dashed curve in Fig. 2 is the theoretical curve for the conductivity mobility of sample 1, calculated in the same way. The electron density used was 3.5×10^{15} cm^{-3} and N_I was determined from the fit of the theoretical curve to the experimental data. The agreement between theory and experiment is not as good as it was for sample 2. This is not surprising, since the Born approximation is not well justified in sample 1 below about 10°K. In sample 2, on the other hand, the Born approximation applies for the range of temperature in this experiment. The solid curve for sample 1 uses a value of K_s, that is, 0.5 the value obtained using the actual carrier density. N_I is unchanged. The better agreement with the smaller K_s probably reflects the failure of the Born approximation. However, we may speculate that the high-impurity density in this sample causes an increase in the density of states near the bottom of the conduction band.[25] This increase in the density of states has the effect of decreasing the mobility at low temperature below the value calculated assuming no effect of the impurities on the density of states. In this case, the K_s calculated from the correct n should give a mobility value in closer agreement with experiment.

Since there is no donor deionization in sample 1, the temperature dependence of R_H cannot be used to determine the donor density N_D and the acceptor density. Instead, we determine N_D and N_A from the ionized-impurity density required to match the theory to the μ_c data. We found that $N_I=(1.1\text{–}1.4)\times10^{16}$ cm^{-3}. The spread is for the two choices of K_s. If we assume that the scattering is due to the ionized donors and acceptors, then we estimate, using 3.5×10^{15} cm^{-3} for the free-electron density, that N_D is $(7.3\text{–}8.8)\times10^{15}$ cm^{-3} and N_A is $(3.8\text{–}5.3)\times10^{15}$ cm^{-3}.

2. Hall Constant

The temperature dependence of the Hall constant for sample 2 (Fig. 1) is typical of an extrinsic semiconductor. The rapid decrease in $(R_He)^{-1}$ below 20°K is due to donor deionization and the minimum in $(R_He)^{-1}$ represents the transition to impurity conduction.[24] Impurity conduction in GaAs has been studied in detail by other authors.[6,26–29] The theoretical curve was calculated assuming only the conduction band contributed to the current. Therefore, the departure of the data points from the curve below 6°K are due to the transition to impurity conduction. The theoretical curve was determined from a least-squares fit of the standard expression[30] for the temperature dependence of the carrier density of an extrinsic semiconductor. Values of $\mu_H\mu_c^{-1}$ were calculated as outlined above, and used to relate n to R_H. For this sample, N_D is 1.3×10^{15} cm^{-3}, N_A is 1.7×10^{14} cm^{-3}, and the donor binding energy $\mathcal{E}_d$ is 0.0036 eV. In making this analysis, a donor level degeneracy of 2 was assumed. At the temperature of the maximum of R_H the impurity- and conduction-band conductivities are equal.[24] From this, we estimate that the impurity mobility is about 6 cm^2 V^{-1} sec^{-1}.

The temperature dependence of $(R_He)^{-1}$ for sample 1 resembles the curve for sample 2, although the decrease is very much smaller and the minimum is at a much higher temperature. It may be tempting to assume, as is usually done,[6,26–29] that the curve for sample 1 is evidence for impurity-band conduction. If we make this assumption, we can, as we did in sample 2, estimate the impurity-band mobility. We conclude that the impurity-band mobility is about 20 000 cm^2 V^{-1} s^{-1}. This value is nearly as high as the conduction-band mobility in sample 2 at 40°K. It is not physically reasonable that the impurity-band mobility should be this high. In sample 2 it was nearly four orders of magnitude less.

If, on the other hand, we assume that all the conduction takes place in the conduction band, we can obtain a consistent picture of the transport. The variation of the ratio $\mu_H\mu_c^{-1}$ with temperature can account for all of the temperature dependence of R_H. This ratio

[20] E. D. Palik, S. Teitler, and R. F. Wallis, J. Appl. Phys. Suppl. **32**, 2132 (1961).
[21] K. Hambleton, C. Hilsum, and B. Holeman, Proc. Phys. Soc. (London) **77**, 1147 (1961).
[22] T. B. Bateman, H. J. McSkimin, and J. M. Whelan, J. Appl. Phys. **30**, 544 (1959).
[23] E. J. Charlson and G. Mott, Proc. IEEE **51**, 1239 (1963); M. Zerbst and H. Boroffka, Z. Naturforsch. **18a**, 642 (1963).
[24] N. F. Mott and W. D. Twose, Advan. Phys. **10**, 107 (1961).
[25] E. O. Kane, Phys. Rev. **131**, 79 (1963).
[26] J. Basinski and R. Olivier, Can. J. Phys. **45**, 119 (1967).
[27] O. V. Emel'yaneko, T. S. Lagunova, D. N. Nasledov, and G. N. Talalakin, Fiz. Tverd. Tela **7**, 816 (1965) [English transl.: Soviet Phys.—Solid State **7**, 1063 (1965)].
[28] D. V. Eddolls, Phys. Status Solidi **17**, 67 (1966).
[29] L. Halbo and R. J. Sladek, Phys. Rev. **113**, 794 (1968).
[30] Reference 1, p. 47.

changes with temperature because of the changes in the scattering mechanisms and the value of the Fermi energy.[15] The curve through the data for sample 1 in Fig. 1 is obtained using Eq. (1) with $n=3.5\times10^{15}$ cm^{-3} and theoretical values of $\mu_H\mu_c^{-1}$. The ratio $\mu_H\mu_c^{-1}$ was calculated as outlined above. The portion of the curve between room temperature and 100°K was not calculated, but extrapolated. Since optical-phonon scattering is important in this region, we could not easily calculate $\mu_H\mu_c^{-1}$.[13] Nevertheless, since $\mu_H\mu_c^{-1}\sim1$ for polar optical-phonon scattering,[31] we set $\mu_H\mu_c^{-1}=1$ at room temperature and made a smooth extrapolation between 100 and 300°K. From the above discussion, we see that the experimental results can be explained without introducing the notion of conduction in an impurity band distinct from the conduction band. There are at least two reasons that evidence for an impurity band was not found. The screening of the donor potential by the conduction-band electrons might preclude donor deionization.[32] The high donor density may cause the donor levels to merge with the conduction band.[33] The latter would have the effect of increasing the conduction-band density of states near the bottom of the band. Corroborative evidence for our model has been given by Eddolls[28] who has shown that the binding energy of the shallow donor in epitaxially grown GaAs extrapolates to zero at a donor density of 10^{16} cm^{-3}. Thus, the absence of freeze-out in sample 1 with a donor density of nearly 10^{16} cm^{-3} is consistent with Eddolls's work.

B. Non-Ohmic Transport

The field dependence of the mobility shown in Figs. 3 and 4 is similar to that observed in GaAs,[5–7] Ge,[1,4] InSb,[34] and CdS.[35,36] There is a similarity among these materials because the mobility is determined by ionized-impurity scattering whose strength decreases with increasing electron energy. Therefore, as the electric field increases the electron energy, the mobility increases. The rapid mobility rise ends, however, when optical-phonon emission dominates the electron transport

To go further than the above qualitative discussion of non-Ohmic transport, we must consider the important electron-scattering mechanisms and asses their roles by comparing theory and experiment. There are two general approaches to non-Ohmic transport. The most widely used method is the ETM, using a shifted Boltzmann or Fermi distribution.[9] However, this approximation is only justified for carrier densities sufficiently high that the electron distribution is determined by electron-electron scattering.[9,37] Certainly, the correct way to treat non-Ohmic transport is to calculate the electron distribution from an exact solution of the transport equation. However, the Boltzmann transport equation has not been solved in general but only approximately in special cases.

Since we found that the ETM could not adequately explain our results, we used the BES approach. This calculation was carried out in an earlier paper.[11] For the treatment of the data, we have extended the theory to include Fermi statistics and screening of the electron-phonon interaction. These modifications are outlined in the Appendix. We shall, therefore, analyze the non-Ohmic transport with a theory that includes ionized impurities and acoustic phonons interacting via both the piezoelectric and deformation potentials. The interactions that are neglected but which might be important in shaping the distribution function are optical-phonon scattering, electron-electron scattering, impact ionization of the donors, and the change of the phonon distribution.[38] The inclusion of these effects presents enormous computational difficulties making their treatment beyond the scope of this paper. We shall attempt to see how well the theory in its present form can explain the experimental results.

Perhaps the clearest method of presentation of non-Ohmic transport is to consider the electron distribution function. In Fig. 6 the number density $dn/d\epsilon$ is plotted versus electron energy $\mathcal{E}$. This quantity is the product of the symmetric part of the distribution function and the square root of the dimensionless energy parameter $\epsilon=\mathcal{E}/kT$. Equation (A1) was used to calculate $dn/d\epsilon$. The solid line is calculated by the BES method. The dashed line is for the ETM using Fermi statistics. Both distributions have an average energy of 5.85 kT and correspond to sample 1 at a lattice temperature of 4.23°K and an electric field of 5 V cm^{-1}. There are two important differences between the two curves. The maximum of $dn/d\epsilon$ is slightly shifted from the Ohmic value of $\epsilon=0.5$ for the case of BES model; whereas, for the ETM the maximum is at $\epsilon=2.93$. The other difference is the long tail in the number density for the BES model. This tail, which contains a small fraction of the free electrons, makes a large contribution to the current.[11] We can understand these differences in the two distribution functions when we consider that the mobility is determined by ionized-impurity scattering, whereas the energy loss is to acoustic phonons (the electron-phonon interaction is primarily via the piezoelectric potential). Since the ionized-impurity scattering time increases roughly as the cube of the electron velocity v [Eq. (2)], the rate of energy gain from the electric field increases as roughly v^3. The energy loss rate to the acoustic phonons increases only linearly

[31] F. Garcia-Molinar, Phys. Rev. **130**, 2290 (1963).
[32] S. P. Li, W. F. Love, and S. C. Miller, Phys. Rev. **162**, 728 (1967).
[33] N. F. Mott, Phil. Mag. **6**, 287 (1961); Can. J. Phys. **34**, 1356 (1956).
[34] H. Miyazawa and H. Ikoma, J. Phys. Soc. Japan **23**, 290 (1967).
[35] M. Saitoh, J. Phys. Soc. Japan **21**, 2540 (1966).
[36] R. S. Crandall, Phys. Rev. **169**, 577 (1968).
[37] A. Hasegawa and J. Yamashita, J. Phys. Soc. Japan **17**, 1751 (1962).
[38] Reference 2, pp. 127–149.

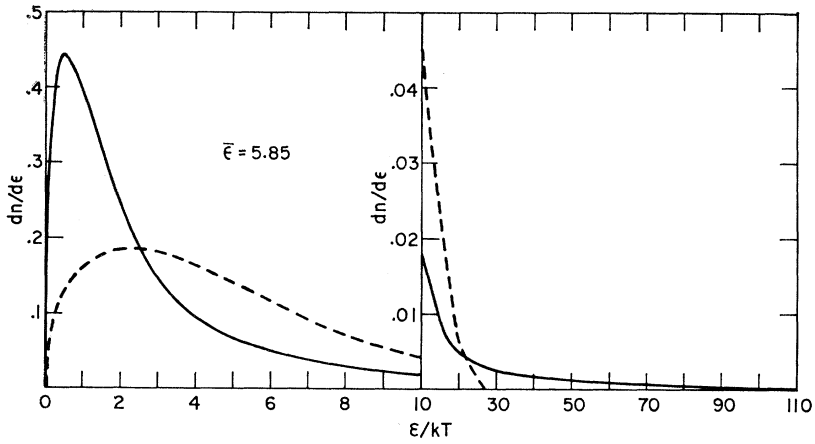

FIG. 6. The number density $dn/d\epsilon$ versus normalized energy $\epsilon = \mathcal{E}/kT$ for the ETM and BES models at an average energy of $5.85kT$. The parameters correspond to sample 1 at a lattice temperature T is 4.23°K and electric field of 5 V cm^{-1}. The solid line is from the BES calculation; the dashed line is the ETM. The tails of the distributions are shown by the scale at right. Note the scale change at $\epsilon = 10$.

with velocity. Therefore, electrons in the tail of the distribution gain energy faster than they lose it and accelerate to higher energy. What keeps the electrons from "running away" is the deformation-potential interaction. At energies above about 0.009 eV ($\sim 20kT$ for Fig. 6) the deformation-potential interaction dominates and the energy loss rate increases as v^3. If we had considered only ionized-impurity scattering and the deformation potential e-p interaction, the distribution function would remain nearly Maxwellian. The long tail would be absent, because there would be no unstable state for the high-velocity electrons. This is the reason that the electron temperature model works so well in germanium.[1,2]

We shall discuss the data for sample 1 first because the field dependence of R_H is caused by the tail on the distribution function. The curves in Fig. 3 are calculated from the BES. For the solid curves the value of K_s that gave the best fit to the Ohmic transport was used. The field dependence of the mobility is not changed significantly by using the correct value of K_s. This is because the field dependence of the mobility is determined mainly by the tail of the distribution which is insensitive to the choice of K_s. This theory can be used to explain the field dependence of the conductivity mobility reasonably well below 5 V cm^{-1}. Above this field, the theory is inappropriate because it predicts that a significant fraction of the electrons are at energies where scattering due to optical-phonon emission should be important. The solid portions of the curves in Fig. 3 are for fields where electrons of energy greater than the optical-phonon energy do not contribute to the calculated current or energy. In the region represented by the broken portions of the curves, up to 5% of the total number of electrons can emit optical phonons. Since these electrons lose most of their energy and momentum by optical-phonon emission, they do not contribute significantly to the current. We have, therefore, approximated optical-phonon scattering in our theory by omitting any contribution to the current by those electrons whose energy is greater than the optical-phonon energy. We used this procedure to calculate the broken portions of the curves in Fig. 3. Of course, this procedure is inappropriate when these optical-phonon scattered electrons become a sizeable fraction of the total electron density. This approach does indicate when optical-phonon emission becomes important. The experimental and theoretical terminations of the rapid mobility rise are in good agreement.

In Fig. 3, for data spanning a factor of 20 in temperature, the mobility and Hall constant above 6 V cm^{-1} are independent of temperature. Above 6 V cm^{-1}, the mobility increases slowly with field until at about 80 V cm^{-1} it begins to decrease with increasing electric field. The independence of the mobility on lattice temperature can be understood to occur once the electron energies are high enough to involve only impurity scattering and phonon emission. The rather weak dependence on electric field ($6 < E < 100$ V cm^{-1}) must be due to a balance between these two different processes. Above 100 V cm^{-1}, where the electrons interact mainly with optical phonons, the phenomenon of the saturated drift velocity occurs.[1,2]

Perhaps, because the function $\mu_H\mu_c^{-1}$ is more sensitive to the shape of the distribution function than is μ_c, the theoretical fit to the ratio $\mu_H\mu_c^{-1}$ in Fig. 3 is not nearly as good as the fit to μ_c. The Hall mobility depends on the average of the square of the scattering time $\langle\tau_s^2\rangle$ whereas μ_c depends on $\langle\tau_s\rangle$. Because τ_s increases with increasing energy, the average of τ_s^2 weights the tail of the distribution more heavily than does $\langle\tau_s\rangle$. Therefore, as the tail of the distribution increases with increasing electric field, we find that $\mu_H\mu_c^{-1} = \langle\tau_s^2\rangle\langle\tau_s\rangle^{-2}$ increases. We can speculate that $\mu_H\mu_c^{-1}$ decreases at high fields because the distribution function changes from one that is spread out in energy to one that has most of the electrons concentrated just below the optical-phonon energy. Since this distribution occupies a narrow range in energy space, $\mu_H\mu_c^{-1}$ approaches unity. In Fig. 3, the $\mu_H\mu_c^{-1}$ data at high fields are virtually independent of temperature and nearly unity. The dashed line at 1.22°K is for the screen-

ing wave vector that applies for the actual carrier density. The solid line is for the value that gave the best fit to the temperature dependence of the mobility. We show both curves to point out how sensitive the field dependence of the ratio $\mu_H\mu_c^{-1}$ is to the value of K_s. The correct value of K_s gives the better fit to the non-Ohmic transport, whereas the K_s value that gives the better fit to the Ohmic transport gives the poorer fit to the non-Ohmic transport. A reason for this is that the Born approximation is better for the high-energy electrons responsible for the non-Ohmic effects than for the low-energy electrons involved in Ohmic transport.

The non-Ohmic transport in Sample 2 is complicated because the carrier density increases in the hot-electron region. This increase is due to a change in the free-electron lifetime caused by the change in the electron distribution,[39] as well as to impact ionization of donor electrons.[40] We believe that impact ionization is the important process because of the rapid carrier increase observed with small changes in the applied field (Fig. 5). Electron density changes due to changes in the carrier lifetime are usually weak functions of the field, since lifetime changes depend on variations of the average electron energy.[39]

This increase in the carrier density has an important effect on the mobility because of the increase in the screening. The increased screening produces a decrease in the ionized-impurity scattering and a decrease in the e-p interaction leading to a hotter electron distribution. Since this hotter distribution produces more impact ionization, a positive feedback occurs. Therefore, the electric field decreases while the distribution remains hot, maintaining the original rate of impact ionization. This feedback phenomenon is the well-known current-controlled negative differential resistance (NDR). The effect was first seen in Ge[41] and recently in GaAs.[5,6,10] Other models for the NDR have been proposed.[42–45]

We tested our model by calculating the field dependence of the Hall mobility for sample 2 at 5.12°K (Fig. 4). In carrying out the calculations, we did not include any effect of impact ionization on the distribution function. As Yamashita[45] pointed out, this may not be a serious omission. The agreement with the data is surprisingly good considering the incompleteness of the model and the hot-electron theory. The agreement between theory and experiment may be fortuitous because the interpretation of the measurement of μ_H in the NDR region is open to question. It is possible that the current flow is filamentary[46] in the NDR region. In this case the μ_H values, assuming homogeneous current flow through the sample, will be in error. With the above in mind we still feel, however, that the theoretical result does show that screening can lead to a NDR.

Note added in proof. A more complete discussion of screening and negative resistance will be published in J. Phys. Chem. Solids.

In sample 2 we did not observe any electric field dependence of the Hall constant at 77°K. The high-field mobility at 77°K is less than at low temperatures because of the increased scattering due to optical-phonon absorption. On comparing the high-field regions (above 4 V cm^{-1}) for the different samples, we see that the purer samples have higher mobilities. This result is expected because even though optical-phonon emission dominates the energy loss process, the momentum relaxation is still dependent on impurity scattering. Even at high fields where the drift velocity is beginning to saturate, the purest sample has the highest drift velocity.

To fit the above data, we used values of the piezoelectric stress constant h_{14} in the range 1.9–2.3×10^9 V m^{-1}. The measured value is 1.57×10^9 V m^{-1}. There is a range in values of h_{14} because we chose the value of h_{14} for each sample and temperature that gave the best fit to experiment. Considering the approximations in the theory, there is good agreement between the measured value of h_{14} and h_{14} determined from non-Ohmic transport. For the deformation potential interaction we used 7 eV, which is the value deduced by Ehrenreich.[13] From a comparison of our theory to experiment, this quantity can be determined only within a factor of 2. If the screening of the electron-phonon interaction is not included, then the value of h_{14} required to fit the data in sample 1 must be chosen 70% weaker and would be at variance with the measured value.

V. SUMMARY

We have shown that low-temperature low-field non-Ohmic transport in GaAs can be explained reasonably well by a theory that includes only scattering by ionized-impurities and acoustic phonons. To make a consistent interpretation of samples with different carrier concentrations, we have had to include screening of the electron-phonon interaction. The electron temperature model was found to give a poor fit to the data, whereas the solution of the Boltzmann equation gave satisfactory agreement with the data. A model which depended upon screening of ionized-impurity and phonon-scattering was proposed for the observed current-controlled negative resistance.

[39] M. Lax, Phys. Rev. **119**, 1502 (1960).
[40] S. H. Koenig, R. D. Brown, III, and W. Schillinger, Phys. Rev. **128**, 1668 (1962).
[41] A. L. McWhorter and R. H. Rediker, Proc. IRE **47**, 1207 (1959).
[42] A. L. McWhorter and R. H. Rediker, in *Proceedings of the International Conference on Semiconductor Physics Prague, 1960* (Academic Press Inc., New York, 1961), p. 134.
[43] T. Kurosawa, J. Phys. Soc. Japan **20**, 1405 (1965).
[44] A. Zylberztejn, J. Phys. Chem. Solids **23**, 297 (1962).
[45] J. Yamashita, J. Phys. Soc. Japan **16**, 720 (1961).
[46] B. K. Ridley, Proc. Phys. Soc. (London) **82**, 954 (1963).

ACKNOWLEDGMENTS

I am indebted to Dr. Ronald Enstrom and John Appert for growing the samples. Dr. Lionel Friedman, Dr. Albert Rose, and Dr. Allen Rothwarf contributed to fruitful discussions. Peter Gwozdz was invaluable in carrying out some of the measurements and programming the analysis of the temperature dependence of the carrier density. My thanks are due Dr. Maurice Glicksman for a critical reading of the manuscript.

APPENDIX

We shall outline the steps in extending the theory developed in I to include Fermi statistics and screening of the electron-phonon interaction.

To include Fermi statistics in the transition from the state K' to the state K we multiply $f(K')$ by the term $1-f(K)$ to ensure that the state K is unoccupied. Thus, on the right-hand side of Eqs. (I-9) and (I-10) we multiply $f(K)$ by $1-f(K')$ and similarly for $f(K')$. The Boltzmann equation is now nonlinear because of the addition of terms involving $f(K)\ f(K')$. When the steps between Eqs. (I-10) and (I-14) are carried out, we find that the only change is that $f(\mathcal{E})$ is multiplied by $1-f(\mathcal{E})$ in Eqs. (I-14) and (I-16). To arrive at this form, terms of the order $f(\mathcal{E})G(\mathcal{E})K$ and higher order were neglected. If we write the integral in (I-17) as $I(\mathcal{E},E)$, the expression for $f(\mathcal{E})$ becomes

$$f(\mathcal{E})=1/[1-N\exp I(\mathcal{E},E)], \tag{A1}$$

where N is a constant to be determined from boundary conditions. If the electric field is zero, $I(\mathcal{E},0)=\mathcal{E}/kT$ and $f(\mathcal{E})$ is the Fermi function. Thus, at zero field, $N=\exp(-\mathcal{E}_F/kT)$, where $\mathcal{E}_F$ is the Fermi energy. The Fermi energy is determined from

$$\int_0^\infty f(\mathcal{E})\mathcal{E}^{1/2}d\mathcal{E}=(2\pi^2\hbar^3/(2m)^{3/2})n. \tag{A2}$$

For finite fields in the limit $\mathcal{E}\to 0$, $I(\mathcal{E},E)$ is the same as the zero-field case. This boundary condition shows that N is the thermal equilibrium value. The remaining equations in I apply with Eq. (A1) for $f(\mathcal{E})$.

To include screening of the e-p interations we shall make the assumption that the Thomas-Fermi expression is a good approximation to screening by conduction-band electrons. For the piezoelectric interaction screening is included by multiplying the interaction potential by

$$q^2/(q^2+K_s^2), \tag{A3}$$

where q is the phonon wave vector. The terms F_0 and F_i, defined in the Appendix of I, become modified by the inclusion of the square of expression (A3) in the integrals. These expressions are lengthy because of the anisotropy of the scattering. Since the scattering anisotropy is a small effect compared to the other errors in the calculation, we shall assume isotropic scattering in treating the screening term. Then F_0 and F_i are multiplied by

$$1-\frac{K_s^2}{2K^2}\ln\left(1+\frac{4K^2}{K_s^2}\right)+\frac{1}{(1+4K^2/K_s^2)}. \tag{A4}$$

For the screened deformation potential interaction, we use expression (5.6.10) given by Ziman.[47] Since the Fermi energy is much less than the deformation potential, this expression reduces to the usual expression for the deformation potential in semiconductors, but multiplied by expression (A3). Therefore, whenever D^2 occurs in I, it should be multiplied by

$$1-\frac{K_s^2}{K^2}+\frac{3K_s^4}{8K^4}\ln\left(1+\frac{4K^2}{K_s^2}\right)-\frac{K_s^2}{2K^2[1+4K^2/K_s^2]}. \tag{A5}$$

In the high-energy limit ($K/K_s\gg 1$) both screening expressions tend to unity. Therefore, we have the unscreened case derived in I. In the low-energy limit, the dependence is as K^4.

In the calculation of $f(\mathcal{E})$, using the above screening expressions, we assume that K_s has the usual form derived for an equilibrium distribution. Actually the problem should be solved self-consistently with the form of K_s determined from the nonequilibrium distribution function. There is, however, some justification for our approximation. The nonequilibrium distribution still has most of the electrons in a distribution that is similar to the equilibrium one. The few electrons in the tail of the distribution contribute little to the screening.

[47] J. M. Ziman, *Electrons and Phonons* (Clarendon Press, Oxford, 1960).